SLAC–PUB–8721
Nov 2000

Z-Quark Coupling Measurements at SLD*

Thomas Wright
University of Wisconsin, Madison, WI 53706

Representing the SLD Collaboration**
Stanford Linear Accelerator Center
Stanford University, Stanford, CA 94309

Abstract

The SLD experiment at SLAC has performed several precise tests of the electroweak Standard Model. This paper summarizes the measurements of Z couplings to quarks. Most of these measurements are preliminary and many incorporate the full SLD dataset of 550,000 polarized Z decays.

Presented at the Meeting of the Division of Particles and Fields
of the American Physical Society
Columbus, Ohio
August 9-12, 2000

*Work supported by Department of Energy contract DE–AC03–76SF00515.

1 Introduction

In the Standard Model, the coupling of a Z to a fermion-antifermion pair is described by a vertex factor:

$$\frac{-ig}{2\cos\theta_W}\gamma^\mu(c_V - c_A\gamma^5) \tag{1}$$

where g is the electroweak coupling constant, θ_W is the electroweak mixing angle, c_V is the vector coupling, and c_A is the axial-vector coupling. The couplings can also be expressed in terms of left- and right-handed couplings and are predicted by the Standard Model:

$$c_V = c_L + c_R = I_3 - 2Q\sin^2\theta_W \tag{2}$$

$$c_A = c_L - c_R = I_3 \tag{3}$$

here Q is the fermion charge and I_3 is the third component of the fermion weak isospin.

The Z-pole observables R_f and A_f can be written in terms of these couplings. R_f is defined as the rate of production of quark flavor f as a fraction of the total hadronic width.

$$R_f = \frac{\Gamma(Z \to f\bar{f})}{\Gamma(Z \to \text{hadrons})} \sim (c_L^f)^2 + (c_R^f)^2 \tag{4}$$

A_f represents the amount of parity violation at the $Zf\bar{f}$ vertex.

$$A_f = \frac{2c_A^f c_V^f}{(c_A^f)^2 + (c_V^f)^2} = \frac{(c_L^f)^2 - (c_R^f)^2}{(c_L^f)^2 + (c_R^f)^2} \tag{5}$$

The Standard Model predictions for A_f for the fermion families are given in Table 1. The lepton asymmetries are seen to be sensitive probes of the electroweak mixing angle $\sin^2\theta_W$. For the quarks, the b system is particularly interesting. Since $(c_L)^2 \sim 30(c_R)^2$, measurements of R_b and A_b correspond to nearly independent determinations of c_L and c_R. Precise measurements of A_f for the different fermions test the universality of the theory between the generations within each family.

Table 1: Coupling parameters and asymmetries for the fermion families.

fermion	I_3	Q	c_L	c_R	A_f	$\frac{dA_f}{d\sin^2\theta_W}$
ν_e, ν_μ, ν_τ	1/2	0	0.50	0.00	1	0
e, μ, τ	-1/2	-1	-0.27	0.23	0.155	-7.9
u, c, t	1/2	2/3	0.35	-0.15	0.667	-3.5
d, s, b	-1/2	-1/3	-0.42	0.08	0.935	-0.6

The Born-level differential cross section for $e^+e^- \to Z \to f\bar{f}$, for longitu-

dially polarized electrons and unpolarized positrons is:

$$\frac{d\sigma}{d\cos\theta_f} \sim (1 - A_e P_e)(1 + \cos^2\theta_f) + 2A_f(A_e - P_e)\cos\theta_f \tag{6}$$

where θ_f is the polar angle of the outgoing fermion with respect to the direction of the incoming electron beam, and P_e is the electron beam polarization. It is possible to isolate the various parameters in Eq. 6 by forming asymmetries in $\cos\theta_f$ and P_e.

The forward-backward asymmetry (for unpolarized beams) is defined as:

$$A_{FB} = \frac{\sigma_F - \sigma_B}{\sigma_F + \sigma_B} = A_e A_f \frac{2\cos\theta}{1 + \cos^2\theta} \tag{7}$$

where F refers to $\cos\theta > 0$. This isolates a combination of the inital- and final-state asymmetries. With a polarized beam it is possible to isolate A_f alone by forming the left-right-forward-backward double asymmetry:

$$\tilde{A}_{FB} = \frac{\sigma_{LF} - \sigma_{LB} - \sigma_{RF} + \sigma_{RB}}{\sigma_{LF} + \sigma_{LB} + \sigma_{RF} + \sigma_{RB}} = |P_e| A_f \frac{2\cos\theta}{1 + \cos^2\theta} \tag{8}$$

Measuring $\tilde{A}_{FB}$ permits a direct measurement of the final-state coupling asymmetry A_f, independent of A_e. This method also has a statistical advantage of $(P_e/A_e)^2 \sim 25$ compared to A_{FB}.

2 The SLD experiment at SLC

The SLAC Linear Collider (SLC) delivered excellent performance in the 1997-98 run, reaching peak luminosities of $3 \times 10^{30} \mathrm{cm}^{-2}\mathrm{s}^{-1}$. Approximately 350,000 Z decays were collected, more than doubling the SLD data set to a total of around 550,000 for 1993-98.

Two features of the SLC make it a good laboratory for electroweak measurements. The first is the highly polarized electron beam. During the 1997-98 run the average longitudinal beam polarization was measured at $72.9 \pm 0.4\%$. The other is the small and stable beam spot ($1.5 \times 0.8 \times 700$ μm), essential for identifying weakly-decaying heavy mesons.

The SLD detector is described in detail elsewhere [1]. One unique feature of the SLD for these measurements is its 3D CCD-based pixel vertex detector (VXD) [2]. In combination with the small SLC beams it allows determination of the interaction point to $4 \times 4 \times 14$ μm, and provides impact parameter resolution of 8×10 μm ($r\phi \times rz$) for high-momentum tracks. Another important component is the Cherenkov Ring Imaging Detector (CRID) [3], which provides good particle identification (particulary $\pi - K$ separation) over a wide momentum range.

3 Quark Couplings

Measurements of the quark couplings require selection of individual flavors from the sample of hadronic Z decays. For bottom and charm events, this is done by searching for displaced secondary vertices resulting from weak decays. The event is split into two hemispheres using the thrust axis, and a topological vertex algorithm [4] is applied to each. The tracks found to originate from displaced vertices, along with any others consistent with the decay chain, are used to calculate a momentum and invariant mass for the hemisphere. The invariant mass is corrected for missing transverse momentum, estimated from the difference between the vertex momentum and flight direction from the IP. These quantities are shown in Figure 1. A typical bottom tag requires $M > 2$ GeV, for 98% purity and 50% efficiency. Charm tagging is done by requiring $0.5 < M < 2$ GeV, $P > 5$ GeV, and $P - 15M > -10$ GeV, for 70% purity and 16% efficiency.

3.1 R_b and R_c

These measurements use a neural network for charm/bottom separation rather than the cuts described above. The mass, momentum, flight distance,

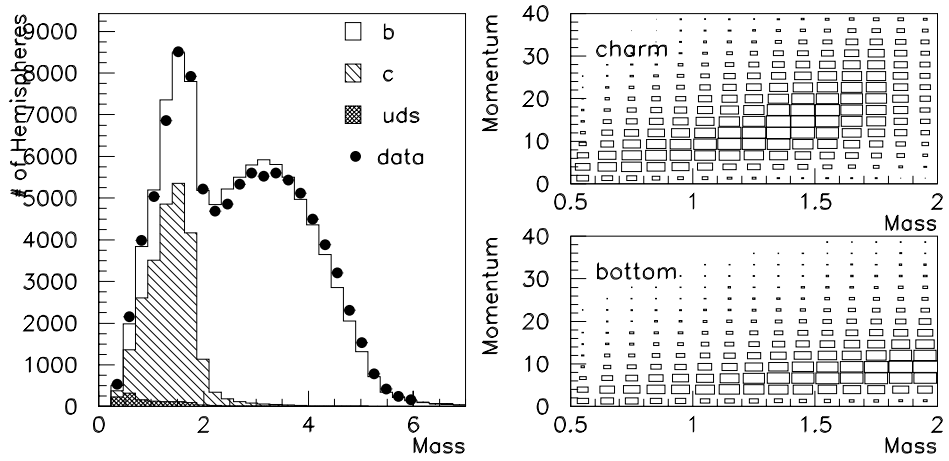

Figure 1: Distributions of M_{VTX} are on the left. The right side shows the correlation between P_{VTX} and M_{VTX} used by the charm tag.

and track multiplicity of the vertex are the input variables. The output of this network is shown in Figure 2. Typical cuts require $NN_{out} > 0.75$ for a bottom-tag and $NN_{out} < 0.3$ for a charm tag. This technique increases the bottom tag efficiency to 62% and the charm tag purity to 85%.

The parameters R_b and R_c are measured using the respective tag rates, but the efficiency must be known. To reduce systematic errors these analyses calibrate it from the data, by measuring the hemisphere tag rate and also

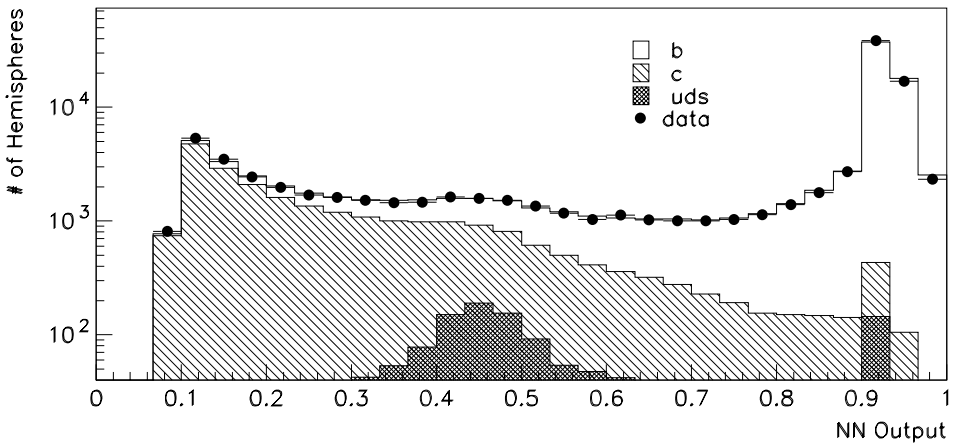

Figure 2: Distributions of the charm/bottom selection neural network output.

the fraction of events which are double-tagged. These can be expressed as:

$$\begin{aligned} F_{hemi} &= \epsilon_b R_b + \epsilon_c R_c + \epsilon_{uds}(1 - R_c - R_b) \\ F_{double} &= \epsilon_b^2 R_b + \epsilon_c^2 R_c + \epsilon_{uds}^2(1 - R_c - R_b) \end{aligned} \tag{9}$$

In the R_b analysis [5], these equations are solved for ϵ_b and R_b. The charm and light-flavor efficiencies are taken from Monte Carlo, and the SM value of R_c is used. A correction for the tag inter-hemisphere correlation is also applied. The preliminary result for the 1993-98 data is $R_b = 0.21669 \pm 0.00094 \pm 0.00101$. For this and the results that follow the first quoted error

is statistical and the second systematic.

The R_c analysis is done in a similar way [5]. In addition to the hemisphere and double-tag rates, the rate to tag one hemisphere of an event with the bottom tag and the other with the charm tag is used, which allows calibration of the b background efficiency. The preliminary result for the 1993-98 data is $R_c = 0.1732 \pm 0.0041 \pm 0.0025$.

3.2 A_{quark} from $\tilde{A}_{FB}$

The heavy-quark asymmetry measurements use the same tags described above to select events. In addition, they must determine which of the hemispheres contains the quark and which the antiquark. The direction of the quark is estimated using the thrust axis, and A_f is extracted from a maximum-likelihood fit to $\tilde{A}_{FB}$. Several techniques are used.

3.2.1 A_b with vertex charge

This measurement uses the total charge of the tracks in the secondary vertex of tagged hemispheres [6]. Correct track assignment is critical, so this analysis attaches tracks using a neural-net algorithm for greater efficiency. Because not all particles are reconstructed in the drift chamber, this analysis also

examines $\geq$ 3-hit vectors in the vertex detector to see if any are consistent with the decay chain. The charge of these can be determined by fitting a helix to the VXD hits and the vertex position, and is correct $\sim$85% of the time. The effect of including these vectors is shown in Figure 3. The analyzing power for bottom events is calibrated from the data, using double-tagged events. Figure 4 shows the polar angle distributions of the signed thrust axis for left- and right-handed electron beams. The preliminary result for 1997-98 data is $A_b = 0.926 \pm 0.019 \pm 0.027$.

3.2.2 A_b with jet charge

This measurement uses the sum of the track charges in each hemisphere, with each track weighted by the square root of the dot-product of its momentum with the thrust axis [7]. Because both hemispheres are always used this analysis benefits from high statistics. The analyzing power for bottom events is calibrated from the data. The preliminary result for 1993-98 data is $A_b = 0.882 \pm 0.020 \pm 0.029$.

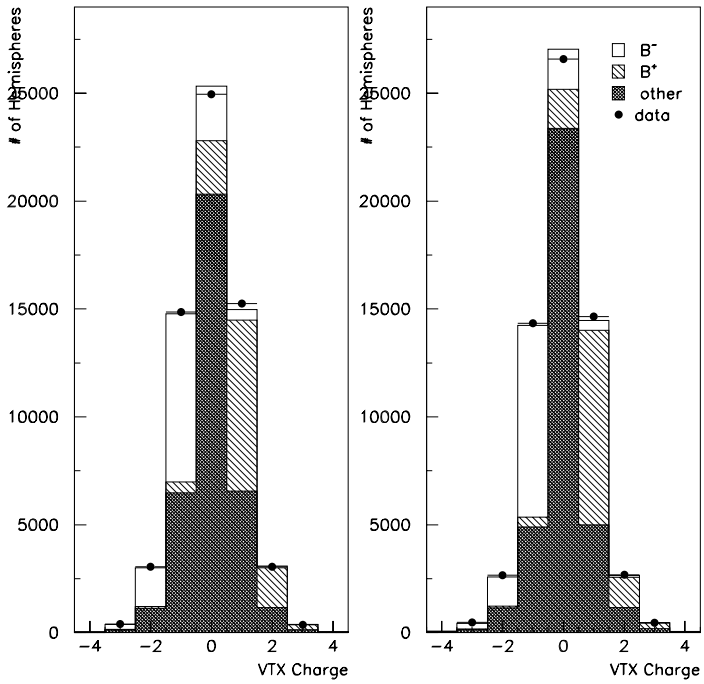

Figure 3: Vertex charge distributions, for only tracks (left) and including VXD vectors (right).

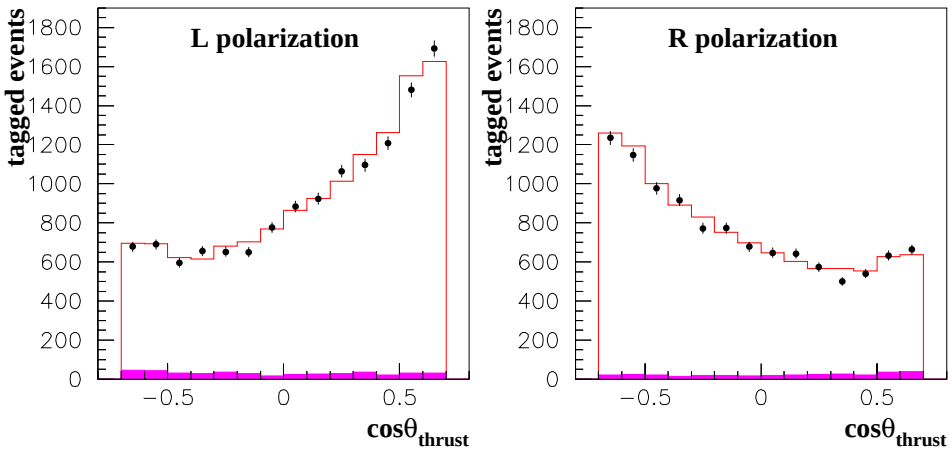

Figure 4: Polar angle distributions of the signed thrust axis for left- and right-handed electron beams. The data are represented by the points, the open histogram is the Monte Carlo reweighted to the same asymmetry, and the solid histogram is the estimated background.

3.2.3 A_b with kaons

This measurement uses charged kaons from the $b \to c \to s$ cascade to tag the b quark [8]. The kaons are identified using the CRID, and only tracks which are attached to a secondary vertex are considered. The analyzing power for bottom events is calibrated from the data using double-tagged events. The preliminary result for 1993-98 data is $A_b = 0.960 \pm 0.040 \pm 0.069$.

3.2.4 A_b and A_c with leptons

These measurements use semileptonic decays of bottom and charm hadrons to tag the quark hemisphere [9]. The electron and muon identification is done using the SLD calorimeters and information from the CRID. Discrimination between b-prompt, b-cascade, and c-prompt decays uses the total and transverse momentum of the lepton. Geometrical information from the vertex detector is also used to improve assignment of the lepton track to the proper position in the decay chain. The asymmetry parameters are extracted simultaneously from a likelihood fit. The preliminary results for 1993-98 data are $A_b = 0.922 \pm 0.029 \pm 0.024$ and $A_c = 0.567 \pm 0.051 \pm 0.064$.

3.2.5 A_c with exclusive D mesons

This measurement exclusively reconstructs six modes: $D^+ \to K^-\pi^+\pi^+$, $D^0 \to K^-\pi^+$, and $D^{*+} \to D^0\pi^+_{soft}$ with D^0 decaying into $K^-\pi^+$, $K^-\pi^+\pi^0$, $K^-\pi^+\pi^+\pi^-$, and $K^-l^+\nu_l$ $(l = e, \mu)$ [10]. The efficiency is $\sim$4%, with high purity and analyzing power. The standard bottom tag is used as a veto on the opposite hemisphere to reject b background. The final result for 1993-98 data is $A_c = 0.690 \pm 0.042 \pm 0.021$.

3.2.6 A_c with inclusive soft pions

This measurement uses the soft pion produced in D^* decays to tag the charm quark [10]. These pions have very low transverse momentum with respect to the D^* jet axis. A signal-to-background ratio of 1:2 is obtained by requiring $p_T^2 < 0.01$ GeV^2. The bottom tag is used to reject b background. The final result for 1993-98 data is $A_c = 0.685 \pm 0.052 \pm 0.038$.

3.2.7 A_c with vertex charge and kaons

This measurement uses the inclusive charm tag [11]. At least one hemisphere must be charm-tagged, and neither may be bottom-tagged. Both vertex charge and identified kaons are used for increased efficiency. The charm analyzing power is high (> 0.8) and is calibrated from the data using double-tagged events. The b background level and analyzing power are also calibrated from the data using the mixed charm+bottom-tagged events. The preliminary result for 1993-98 data is $A_c = 0.608 \pm 0.028 \pm 0.023$.

3.2.8 A_s with kaons

This measurement selects strange events using fast kaons [12]. Charged kaons identified with the CRID and reconstructed neutral kaons are used. Both

hemispheres must contain at least one K, with at least one hemisphere having net K charge. Information from the vertex detector is used to suppress the heavy-flavor backgrounds. The final result for 1993-98 data is $A_s = 0.895 \pm 0.066 \pm 0.062$.

Table 2: Summary of SLD electroweak measurements.

R_b	0.2167 ± 0.0014
R_c	0.1732 ± 0.0048
A_b	0.914 ± 0.024
A_c	0.635 ± 0.027
A_s	0.895 ± 0.090

4 Conclusions

SLD has performed several precise tests of the electroweak Standard Model. The results are summarized in Table 2. The R_b and R_c results are in agreement with Standard Model predictions and other measurements at LEP, with the SLD R_c measurement representing the single most precise determination. The combined SLD A_b, A_c, and A_s measurements are also in agreement with

Standard Model predictions. The A_b and A_s measurements support down-type quark universality. Many of these measurements are still in active development. In particular, work is proceeding to reduce the systematic errors on the R_b and A_b measurements.

References

[1] K. Abe *et al.*, Phys. Rev. **D53**, 1023 (1996).

[2] K. Abe *et al.*, Nucl. Inst. Meth. **A400**, 287 (1997).

[3] K. Abe *et al.*, Nucl. Inst. Meth. **A343**, 74 (1994).

[4] D. Jackson, Nucl. Inst. Meth. **A388**, 247 (1997).

[5] K. Abe *et al.*, SLAC-PUB-8667, contributed to ICHEP (2000).

[6] K. Abe *et al.*, SLAC-PUB-8542, contributed to ICHEP (2000).

[7] K. Abe *et al.*, Phys. Rev. Lett. **81** 942 (1998).

[8] K. Abe *et al.*, SLAC-PUB-8200, contributed to EPS-HEP (1999).

[9] K. Abe *et al.*, Phys. Rev. Lett. **83**, 3384 (1999).

[10] K. Abe *et al.*, SLAC-PUB-8447, contributed to ICHEP (2000).

[11] K. Abe *et al.*, SLAC-PUB-8199, contributed to EPS-HEP (1999).

[12] K. Abe *et al.*, SLAC-PUB-8408, (2000).

Acknowledgements

We thank the personnel of the SLAC accelerator department and the technical staffs of our collaborating institutions for their outstanding efforts on our behalf.

*Work supported by Department of Energy contracts: DE-FG02-91ER40676 (BU), DE-FG03-91ER40618 (UCSB), DE-FG03-92ER40689 (UCSC), DE-FG03-93ER40788 (CSU), DE-FG02-91ER40672 (Colorado), DE-FG02-91ER40677 (Illinois), DE-AC03-76SF00098 (LBL), DE-FG02-92ER40715 (Massachusetts), DE-FC02-94ER40818 (MIT), DE-FG03-96ER40969 (Oregon), DE-AC03-76SF00515 (SLAC), DE-FG05-91ER40627 (Tennessee), DE-FG02-95ER40896 (Wisconsin), DE-FG02-92ER40704 (Yale); National Science Foundation grants: PHY-91-13428 (UCSC), PHY-89-21320 (Columbia), PHY-92-04239 (Cincinnati), PHY-95-10439 (Rutgers), PHY-88-19316 (Vanderbilt), PHY-92-03212 (Washington); The UK Particle Physics and Astronomy Research Council (Brunel, Oxford and RAL); The Istituto Nazionale di Fisica Nucleare of Italy (Bologna, Ferrara, Frascati, Pisa, Padova, Perugia); The Japan-US Cooperative Research Project on High Energy Physics (Nagoya, Tohoku); The Korea Research Foundation (Soongsil, 1997).

** List of Authors

Kenji Abe,[15] Koya Abe,[24] T. Abe,[21] I. Adam,[21] H. Akimoto,[21]
D. Aston,[21] K.G. Baird,[11] C. Baltay,[30] H.R. Band,[29] T.L. Barklow,[21]
J.M. Bauer,[12] G. Bellodi,[17] R. Berger,[21] G. Blaylock,[11] J.R. Bogart,[21]
G.R. Bower,[21] J.E. Brau,[16] M. Breidenbach,[21] W.M. Bugg,[23]
D. Burke,[21] T.H. Burnett,[28] P.N. Burrows,[17] A. Calcaterra,[8]
R. Cassell,[21] A. Chou,[21] H.O. Cohn,[23] J.A. Coller,[4] M.R. Convery,[21]
V. Cook,[28] R.F. Cowan,[13] G. Crawford,[21] C.J.S. Damerell,[19]
M. Daoudi,[21] S. Dasu,[29] N. de Groot,[2] R. de Sangro,[8] D.N. Dong,[21]
M. Doser,[21] R. Dubois,[21] I. Erofeeva,[14] V. Eschenburg,[12] S. Fahey,[5]
D. Falciai,[8] J.P. Fernandez,[26] K. Flood,[11] R. Frey,[16] E.L. Hart,[23]
K. Hasuko,[24] S.S. Hertzbach,[11] M.E. Huffer,[21] X. Huynh,[21]
M. Iwasaki,[16] D.J. Jackson,[19] P. Jacques,[20] J.A. Jaros,[21]
Z.Y. Jiang,[21] A.S. Johnson,[21] J.R. Johnson,[29] R. Kajikawa,[15]
M. Kalelkar,[20] H.J. Kang,[20] R.R. Kofler,[11] R.S. Kroeger,[12]
M. Langston,[16] D.W.G. Leith,[21] V. Lia,[13] C. Lin,[11] G. Mancinelli,[20]
S. Manly,[30] G. Mantovani,[18] T.W. Markiewicz,[21] T. Maruyama,[21]
A.K. McKemey,[3] R. Messner,[21] K.C. Moffeit,[21] T.B. Moore,[30]
M. Morii,[21] D. Muller,[21] V. Murzin,[14] S. Narita,[24] U. Nauenberg,[5]
H. Neal,[30] G. Nesom,[17] N. Oishi,[15] D. Onoprienko,[23] L.S. Osborne,[13]
R.S. Panvini,[27] C.H. Park,[22] I. Peruzzi,[8] M. Piccolo,[8] L. Piemontese,[7]
R.J. Plano,[20] R. Prepost,[29] C.Y. Prescott,[21] B.N. Ratcliff,[21]
J. Reidy,[12] P.L. Reinertsen,[26] L.S. Rochester,[21] P.C. Rowson,[21]
J.J. Russell,[21] O.H. Saxton,[21] T. Schalk,[26] B.A. Schumm,[26]

J. Schwiening,[21] V.V. Serbo,[21] G. Shapiro,[10] N.B. Sinev,[16]
J.A. Snyder,[30] H. Staengle,[6] A. Stahl,[21] P. Stamer,[20] H. Steiner,[10]
D. Su,[21] F. Suekane,[24] A. Sugiyama,[15] S. Suzuki,[15] M. Swartz,[9]
F.E. Taylor,[13] J. Thom,[21] E. Torrence,[13] T. Usher,[21] J. Va'vra,[21]
R. Verdier,[13] D.L. Wagner,[5] A.P. Waite,[21] S. Walston,[16]
A.W. Weidemann,[23] E.R. Weiss,[28] J.S. Whitaker,[4] S.H. Williams,[21]
S. Willocq,[11] R.J. Wilson,[6] W.J. Wisniewski,[21] J.L. Wittlin,[11]
M. Woods,[21] T.R. Wright,[29] R.K. Yamamoto,[13] J. Yashima,[24]
S.J. Yellin,[25] C.C. Young,[21] H. Yuta.[1]

(The SLD Collaboration)

[1] *Aomori University, Aomori , 030 Japan,*
[2] *University of Bristol, Bristol, United Kingdom,*
[3] *Brunel University, Uxbridge, Middlesex, UB8 3PH United Kingdom,*
[4] *Boston University, Boston, Massachusetts 02215,*
[5] *University of Colorado, Boulder, Colorado 80309,*
[6] *Colorado State University, Ft. Collins, Colorado 80523,*
[7] *INFN Sezione di Ferrara and Universita di Ferrara, I-44100 Ferrara, Italy,*
[8] *INFN Lab. Nazionali di Frascati, I-00044 Frascati, Italy,*
[9] *Johns Hopkins University, Baltimore, Maryland 21218-2686,*
[10] *Lawrence Berkeley Laboratory, University of California, Berkeley, California 94720,*
[11] *University of Massachusetts, Amherst, Massachusetts 01003,*
[12] *University of Mississippi, University, Mississippi 38677,*
[13] *Massachusetts Institute of Technology, Cambridge, Massachusetts 02139,*

[14] *Institute of Nuclear Physics, Moscow State University, 119899, Moscow*

Russia,
[15] *Nagoya University, Chikusa-ku, Nagoya, 464 Japan,*
[16] *University of Oregon, Eugene, Oregon 97403,*
[17] *Oxford University, Oxford, OX1 3RH, United Kingdom,*
[18] *INFN Sezione di Perugia and Universita di Perugia, I-06100 Perugia, Italy,*
[19] *Rutherford Appleton Laboratory, Chilton, Didcot, Oxon OX11 0QX United Kingdom,*
[20] *Rutgers University, Piscataway, New Jersey 08855,*
[21] *Stanford Linear Accelerator Center, Stanford University, Stanford, California 94309,*
[22] *Soongsil University, Seoul, Korea 156-743,*
[23] *University of Tennessee, Knoxville, Tennessee 37996,*
[24] *Tohoku University, Sendai 980, Japan,*
[25] *University of California at Santa Barbara, Santa Barbara, California 93106,*
[26] *University of California at Santa Cruz, Santa Cruz, California 95064,*
[27] *Vanderbilt University, Nashville,Tennessee 37235,*
[28] *University of Washington, Seattle, Washington 98105,*
[29] *University of Wisconsin, Madison,Wisconsin 53706,*
[30] *Yale University, New Haven, Connecticut 06511.*